

# Solving nonlinear Schrodinger equation using stable implicit finite difference method in single-mode optical fibers

Abeer A. Alanazi<sup>1,2</sup> | Sultan Z. Alamri<sup>1</sup>  | Sharidan Shafie<sup>2</sup> | Shazirawati Binti Mohd Puzi<sup>2</sup>

<sup>1</sup>Department of Mathematics, College of Science, Taibah University, Almadinah, Saudi Arabia

<sup>2</sup>Department of Mathematical Sciences, Faculty of Science, Universiti Teknologi Malaysia, Johor Bahru, Malaysia

## Correspondence

Sultan Z. Alamri, Department of Mathematics, College of Science, Taibah University, Almadinah, Saudi Arabia.  
 Email: appliedmath2020@gmail.com

Communicated by: J. Merker

The different nonlinear Schrodinger equation (NLSE) types describe a lot of interesting physical phenomena. The NLSE which models the light in single-mode nonlinear optical fibers propagation when the wave packet drift and attenuation are neglected has been studied. A stable implicit scheme is developed to solve this equation. The accuracy of this method is second order over both the space and time. By using von-Neumann stability analysis, we have proven that our scheme is unconditionally stable. Numerically, many tests have been proceeded to present the scheme robustness. It is proven that the mass, momentum, and energy are conserved. The interaction between solitons with different directions has been studied. The effects of the factors of chromatic dispersion and self-phase modulation on the solitons movement and conserved quantities as well as the relation between the factors have been discussed. It has been found that the physical parameters of self-phase modulation and chromatic dispersion impacts are beneficial especially for fiber optical investigations.

## KEY WORDS

finite difference method, NLSE, optical fibers, self-phase modulation

## JEL CLASSIFICATION

35A08; 35A20; 35Q51; 35Q55; 65Z05; 78M20

## 1 | INTRODUCTION

New communications technology has become very important according to fiber optical applications in allowing longer transmission distances with higher bandwidths.<sup>1</sup> Today, traveling pulses data in optical fiber transfer the telecommunications bulk of all data. Transmissions in fibers are preferable in comparison to electrical one in cables because of two effective features: waves in fiber suffer low power loss, and fibers supply an extremely wide bandwidth.<sup>2</sup>

The temporal-optical solitonic waves of the nonlinear Schrodinger equation (NLSE) have been investigated theoretically, experimentally, and by simulation to examine its properties in communications using fiber optics.<sup>3–13</sup> Also, these optical fibers are introduced as a serious alternative to next generations in ultrafast telecommunications systems.<sup>3,7,9,13</sup> The nonlinearly forms of NLSE became one of the major delegated ways for depicting the waves behavior in a large number of nonlinear physical applications, that is, plasmas, optics, fluids, deeper water, semiconductors, Bose–Einstein

condensation, and dynamical models.<sup>3–17</sup> Wazwaz and Xu introduce remarks on the optical behavior of bright and dark solitons for NLSE with cubic and log nonlinearity.<sup>11</sup> The unstable nonlinear new solitary characteristics in strong dispersive space and environmental fluids have been investigated to discuss the wave behavior at critical points that existed in the medium in periodic series.<sup>13</sup> Moreover, the NLSE performs a definitely main role in nonlinear applications and studies in fiber optics due to its possessing of soliton solutions.<sup>1,2,18–21</sup> The sine–Gordon and generalized tanh techniques are introduced to obtain the solitary optical solutions to perturbed NLSE (PNLSE). It was noted that the bright, dark, and singularity optical waves are advised to study the behavior dynamics of PNLSE.<sup>14</sup> The NLSE that describes the light progress in single-mode nonlinear optical fibers when the wave packet drift and attenuation are neglected takes the following form:

$$i\frac{\partial\phi}{\partial t} - \frac{\beta}{2}\frac{\partial^2\phi}{\partial x^2} + \gamma|\phi|^2\phi = 0, \quad -\infty < x < \infty, \quad t \geq 0, \quad (1.1)$$

where  $\phi(x, t)$  is the complex slowly varying pulse envelope, ( $\beta \in R - \{0\}$ ) is the chromatic dispersion (CD), ( $\gamma > 0$ ) is the self-phase modulation (SPM), and  $i = \sqrt{-1}$ .<sup>15</sup> The cubic bounded potentials NLSE which describes the optical solitons progress in fibers have been reported by integration constraint conditions on optical parameters required for solitons existence.<sup>18</sup> The multiplier approaches are used to retrieve the NLSE conservation laws. Also, modulation instability calculations for NLSE model are examined using parameter explanation for new physical results interpretation.<sup>18</sup> Furthermore, Houwe et al. investigated chirped soliton properties in the presence of negative indexed, phase modulation and Kerr nonlinearity by solving generalized NLSE with auxiliary equations method.<sup>19</sup> On the other hand, for nonlinear modified Schrodinger's form, the Davydov soliton types have been studied by Lie point symmetries and the corresponding local laws of conservation. Numerical simulations have shown that many solutions given an important physical significance.<sup>22</sup> Also, the nonlinear analysis of Lie symmetries of evolution time fractional dispersion type's equations has been inserted to produce solvable reduced differential equations. Some solutions for the fraction time-reduced equations with Erdelyi–Kober sense derivatives have been numerically used in realization of physical and dynamical applications.<sup>23,24</sup>

Many nonlinear phenomena are described by very complicated and coupled differential equations. Usually, these equations cannot be solved without any approximations. So numerical calculations, methods, and schemes must be taken into account to solve the complicated problems.<sup>25–29</sup> Wu et al. used numerical scheme to study the time Crank–Nicolson accuracy analysis for the very applicable form of diffusion equations.<sup>20</sup> Li et al. tested the space–time order accuracy scheme of Crank–Nicolson (C-N) type to satisfy the conservations of discrete mass. Thomas algorithm enhanced the computational efficiencies of binary collisions and solitary solutions by using random perturbations to the initial conditions.<sup>30</sup> Many researches<sup>3–13</sup> tend to solve the NLSE equation by using different numerical and analytical methods with no focus on the parameters considered in Equation (1.1). Therefore, the main focus of this article is to solve the NLSE numerically by using an implicit finite difference method which is second order in space and time and unconditionally stable. Also, this paper proposes to discuss the effects of the CD,  $\beta$ , and the SPM,  $\gamma$  factors on solitons' movements and on the conserved quantities. These aims are achieved by deriving a computer code by using FORTRAN software, to solve the resulting scheme. Many numerical experiments are studied in the cases of one soliton, two solitons, three solitons, and shock wave. In 1982, Griffiths et al. have studied the NLSE by both the finite element Galerkin and the finite difference numerical methods wherever the former based on linearly elements and product approximations. They reported that the Galerkin technique achieves more accurate and acceptable results. Many physical problems such as the soliton interactions and collisions have been studied.<sup>31</sup>

Taha and Ablowitz used the different numerical method to approximate the NLSE such as the classical explicit, Hopscotch, Crank–Nicolson, implicit–explicit, Ablowitz and Ladik, Fourier, pseudospectral, and split step methods. It was noted that the split step Fourier, pseudospectral, and Ablowitz–Ladik global methods are the best for the NLSE applications.<sup>32</sup> Fadul Albar solved the NLSE with trivial Neumann bounded interval, by using Crank–Nicolson and Newton's methods for the nonlinear system. The produced scheme is second order and unconditionally stable in space and time.<sup>33</sup> Also, different numerical solutions for single soliton and two soliton collisions showed that the energy is conserved. In addition, Douglas idea was used to get a scheme of the fourth order in space, second order in time, and unconditionally stable by the implicit midpoint rule. Then predictor–corrector method was introduced to solve the nonlinear system obtained. The resulting scheme was checked numerically on single soliton, two solitons, and three solitons which proved that the energy is conserved. In the case of two solitons where one of them is faster than the other, through the evolution over time, this study found that the faster soliton passes the slower, which means that

the two solitons exchanged the places.<sup>33</sup> Alamri introduced a numerical scheme to solve the CNLSE in one dimension using Crank–Nicolson method and found that the method is unconditional stable with second-order accuracy of the resulting scheme in space–time.<sup>25</sup> Moreover, this system has been solved using Douglas idea with implicit midpoint rule to get a scheme of fourth-order accuracy in space and second order in time. Also, it was proved that these schemes conserve the mass, momentum, and energy.<sup>25</sup>

## 2 | EXACT SOLUTION

Consider the NLSE of one dimension in single-mode fiber of light propagation:

$$i\frac{\partial\phi}{\partial t} - \frac{\beta}{2}\frac{\partial^2\phi}{\partial x^2} + \gamma|\phi|^2\phi = 0, \quad -\infty < x < \infty, t \geq 0,$$

with the initial condition

$$\phi(x, 0) = g(x), \quad (2.1)$$

and the boundary condition

$$\frac{\partial\phi}{\partial x}(x, t) = 0, \quad \text{at } x \rightarrow \pm\infty, \quad (2.2)$$

where  $\phi(x, t)$  is the complex slowly varying pulse envelope,  $\beta$  is the CD, and  $\gamma$  is the SPM.

To find the exact solution of the NLSE in Equation (1.1), assume that the solution is on the following form:<sup>25,33</sup>

$$\phi(x, t) = u(\chi) \exp\{i(rx - st)\}, \quad \chi = x - ct, \quad (2.3)$$

where  $u(\chi)$  is a real function,  $r$  is the wavenumber,  $s$  is the angular velocity, and  $c$  is the phase velocity. The boundary condition takes the form

$$u(\chi) \rightarrow 0 \quad \text{as } x \rightarrow \pm\infty.$$

Substitute Equation (2.3) into Equation (1.1) to get the following ordinary differential equation:

$$-i(c + \beta r)u' - \frac{\beta}{2}u'' + \gamma u^3 + \left(s + \frac{\beta}{2}r^2\right)u = 0. \quad (2.4)$$

Therefore, the real and imaginary parts can be written as follows:

$$(c + \beta r)u' = 0, \quad (2.5)$$

and

$$-\frac{\beta}{2}u'' + \gamma u^3 + \left(s + \frac{\beta}{2}r^2\right)u = 0. \quad (2.6)$$

In the case of  $\beta < 0$ , let  $-\beta = \beta_1$ , where  $\beta_1 > 0$ ; thus, from Equation (2.5),

$$r = \frac{c}{\beta_1}, \quad (2.7)$$

and Equation (2.6) becomes on the following form:

$$\frac{\beta_1}{2}u'' + \gamma u^3 + \left(s - \frac{\beta_1}{2}r^2\right)u = 0. \quad (2.8)$$

Let  $a$  be the amplitude which can be obtained from the following relation:

$$-a = s - \frac{\beta_1}{2}r^2. \quad (2.9)$$

So the angular velocity  $s$  can be obtained by substituting Equation (2.7) into Equation (2.9) as follows:

$$s = -a + \frac{c^2}{2\beta_1}. \quad (2.10)$$

Then substituting Equation (2.9) into Equation (2.8) gives the following ordinary differential equation:

$$\frac{\beta_1}{2}u'' + \gamma u^3 - au = 0. \quad (2.11)$$

Multiplying Equation (2.11) by  $u'$  and integrating the resulting equation to get the following equation

$$\frac{\beta_1}{4}(u')^2 + \frac{\gamma}{4}u^4 - \frac{a}{2}u^2 + K = 0,$$

where the value of the constant of integration  $k$  can be chosen to be zero, thus, the following equation is obtained

$$\frac{1}{u\sqrt{\gamma}} \frac{du}{\sqrt{u^2 - \frac{2a}{\gamma}}} = \pm \frac{d\chi}{\sqrt{\beta_1}}. \quad (2.12)$$

Solve the differential equation (2.12) in the **positive case** gives by imposing that

$$\begin{aligned} u &= \sqrt{\frac{2a}{\gamma}} \operatorname{sech} \theta, \text{ which implies that} \\ du &= -\sqrt{\frac{2a}{\gamma}} \operatorname{sech} \theta \tanh \theta d\theta. \end{aligned}$$

Therefore, the positive case of the differential equation (2.12) takes the following form:

$$\frac{-1}{\sqrt{\gamma}} \frac{\tanh \theta d\theta}{\sqrt{\frac{2a}{\gamma} - \frac{2a}{\gamma} \operatorname{sech}^2 \theta}} = \frac{d\chi}{\sqrt{\beta_1}},$$

which can be solved as

$$u = \sqrt{\frac{2a}{\gamma}} \operatorname{sech} \left[ \sqrt{\frac{2a}{\beta_1}}(ct - x) \right]. \quad (2.13)$$

By substituting Equations (2.7), (2.10), and (2.13) into Equation (2.3), the exact solution of the NLSE (1.1) takes the following form:

$$\phi(x, t) = \sqrt{\frac{2a}{\gamma}} \operatorname{sech} \left( \sqrt{\frac{-2a}{\beta}} (ct - x) \right) \exp \left\{ i \left[ \left( \frac{-c}{\beta} \right) x + \left( a + \frac{c^2}{2\beta} \right) t \right] \right\}. \quad (2.14)$$

Similarly for **the negative case** of the differential equation (2.12), the other exact solution of the NLSE (1.1) takes the following form:

$$\phi(x, t) = \sqrt{\frac{2a}{\gamma}} \operatorname{sech} \left( \sqrt{\frac{-2a}{\beta}} (x - ct) \right) \exp \left\{ i \left[ \left( \frac{-c}{\beta} \right) x + \left( a + \frac{c^2}{2\beta} \right) t \right] \right\}. \quad (2.15)$$

In the case of  $\beta > 0$  and from Equation (2.5),

$$r = -\frac{c}{\beta}. \quad (2.16)$$

Let  $a$  be the amplitude which can be obtained from the following relation:

$$-a = s + \frac{\beta}{2} r^2. \quad (2.17)$$

Thus, the angular velocity  $s$  can be obtained by substituting Equation (2.16) into Equation (2.17) as follows:

$$s = -a - \frac{c^2}{2\beta}. \quad (2.18)$$

By substituting Equation (2.17) into Equation (2.6),

$$-\frac{\beta}{2} u'' + \gamma u^3 - au = 0. \quad (2.19)$$

Multiplying Equation (2.19) by  $u'$  and integrating the resulting equation gives the following equation:

$$\frac{1}{u\sqrt{\gamma}} \frac{du}{\sqrt{u^2 - \frac{2a}{\gamma}}} = \pm \frac{d\chi}{\sqrt{\beta}}, \quad (2.20)$$

where the value of the constant of integration can be set to be zero. Solve **the positive case** of the differential equation (2.20) to obtain

$$u = \sqrt{\frac{2a}{\gamma}} \sec \left( \sqrt{\frac{2a}{\beta}} (x - ct) \right), \quad (2.21)$$

where the constant of integration was set to zero.

Now, substitute Equations (2.16), (2.18), and (2.21) into Equation (2.3) to obtain the solution of the NLSE (1.1) on the form

$$\phi(x, t) = \sqrt{\frac{2a}{\gamma}} \sec \left( \sqrt{\frac{2a}{\beta}} (x - ct) \right) \exp \left\{ i \left[ \left( \frac{-c}{\beta} \right) x + \left( a + \frac{c^2}{2\beta} \right) t \right] \right\}. \quad (2.22)$$

Next, by solving the differential equation (2.20) in **the negative case** and choosing the constants of integration to be zeroes, the function  $u$  is given as follows:

$$u = \sqrt{\frac{2a}{\gamma}} \sec\left(\sqrt{\frac{2a}{\beta}}(ct - x)\right). \quad (2.23)$$

Now, substitute Equations (2.16), (2.18), and (2.23) into Equation (2.3) to obtain the other solution of the NLSE (1.1) on the form

$$\phi(x, t) = \sqrt{\frac{2a}{\gamma}} \sec\left(\sqrt{\frac{2a}{\beta}}(ct - x)\right) \exp\left\{i\left[\left(\frac{-c}{\beta}\right)x + \left(a + \frac{c^2}{2\beta}\right)t\right]\right\}. \quad (2.24)$$

### 3 | CONSERVATION LAWS

The NLSE (1.1) has some conserved quantities such as mass, momentum, and energy which are indicated in the following relations.<sup>25,26,33</sup>

#### 3.1 | Mass conservation law

$$\int_{-\infty}^{\infty} |\phi|^2 dx = \text{constant}. \quad (3.1)$$

*Proof.* To prove Equation (3.1), assume that the complex wave function  $\phi$  and its complex conjugate are on the form<sup>25,33</sup>

$$\phi(x, t) = v(x, t) + iw(x, t), \quad \bar{\phi}(x, t) = v(x, t) - iw(x, t), \quad (3.2)$$

where  $v(x, t)$  and  $w(x, t)$  are real functions; thus, the boundary condition of Equation (1.1) becomes as follows:

$$\left\{\frac{\partial v}{\partial x}, \frac{\partial w}{\partial x}\right\} \rightarrow 0 \text{ as } x \rightarrow \pm\infty. \quad (3.3)$$

Then, multiply Equation (1.1) by  $\bar{\phi}$  to get the following relation:

$$i\left(\frac{\partial v}{\partial t} + i\frac{\partial w}{\partial t}\right)(v - iw) - \frac{\beta}{2}\left(\frac{\partial^2 v}{\partial x^2} + i\frac{\partial^2 w}{\partial x^2}\right)(v - iw) + \gamma(v^2 + w^2)^2 = 0 \quad (3.4)$$

by taking the imaginary part of Equation (3.4)

$$v\frac{\partial v}{\partial t} + w\frac{\partial w}{\partial t} - \frac{\beta}{2}\left(v\frac{\partial^2 w}{\partial x^2} - w\frac{\partial^2 v}{\partial x^2}\right) = 0,$$

which can be written as follows:

$$\frac{1}{2} \frac{\partial}{\partial t} [v^2 + w^2] - \frac{\beta}{2} \left( v \frac{\partial^2 w}{\partial x^2} - w \frac{\partial^2 v}{\partial x^2} \right) = 0. \quad (3.5)$$

By integrating Equation (3.5) with respect to  $x$  by using integration by parts with the boundary condition in Equation (3.3), the following relation is obtained:

$$\frac{1}{2} \frac{\partial}{\partial t} \int_{-\infty}^{\infty} |\phi|^2 dx = 0,$$

which leads to the following mass conservation law:

$$\int_{-\infty}^{\infty} |\phi|^2 dx = \text{Constant}.$$

### 3.2 | Momentum conservation law

$$i \int_{-\infty}^{\infty} \left( \bar{\phi} \frac{\partial \phi}{\partial x} - \frac{\partial \bar{\phi}}{\partial x} \phi \right) dx = \text{constant}. \quad (3.6)$$

*Proof.* To prove Equation (3.6), multiply the NLSE (1.1) by  $\partial \bar{\phi} / \partial x$  and its complex conjugate by  $\partial \phi / \partial x$  to obtain the following equation:

$$i \frac{\partial \phi}{\partial t} \frac{\partial \bar{\phi}}{\partial x} - \frac{\beta}{2} \frac{\partial^2 \phi}{\partial x^2} \frac{\partial \bar{\phi}}{\partial x} + \gamma \frac{\partial \bar{\phi}}{\partial x} \phi |\phi|^2 = 0, \quad (3.7)$$

$$-i \frac{\partial \phi}{\partial x} \frac{\partial \bar{\phi}}{\partial t} - \frac{\beta}{2} \frac{\partial \phi}{\partial x} \frac{\partial^2 \bar{\phi}}{\partial x^2} + \gamma \bar{\phi} \frac{\partial \phi}{\partial x} |\phi|^2 = 0. \quad (3.8)$$

Then add Equation (3.7) to Equation (3.8) to get the following equation:

$$i \left( \frac{\partial \phi}{\partial t} \frac{\partial \bar{\phi}}{\partial x} - \frac{\partial \phi}{\partial x} \frac{\partial \bar{\phi}}{\partial t} \right) - \frac{\beta}{2} \left( \frac{\partial^2 \phi}{\partial x^2} \frac{\partial \bar{\phi}}{\partial x} + \frac{\partial \phi}{\partial x} \frac{\partial^2 \bar{\phi}}{\partial x^2} \right) + \gamma |\phi|^2 \frac{\partial}{\partial x} (|\phi|^2) = 0. \quad (3.9)$$

After that, differentiate the NLSE (1.1) and its complex conjugate with respect to  $x$  and multiply the former resulting equation by  $\bar{\phi}$  and the latter one by  $\phi$  to get the following correlation:

$$i \phi_{xt} \bar{\phi} - \frac{\beta}{2} \frac{\partial^3 \phi}{\partial x^3} \bar{\phi} + \gamma \left[ |\phi|^2 \frac{\partial}{\partial x} (|\phi|^2) + \bar{\phi} \frac{\partial \phi}{\partial x} |\phi|^2 \right] = 0, \quad (3.10)$$

$$-i\phi \frac{\partial^2 \bar{\phi}}{\partial x \partial t} - \frac{\beta}{2} \phi \frac{\partial^3 \bar{\phi}}{\partial x^3} + \gamma \left[ |\phi|^2 \frac{\partial}{\partial x} (|\phi|^2) + \frac{\partial \bar{\phi}}{\partial x} \phi |\phi|^2 \right] = 0. \quad (3.11)$$

Add Equation (3.10) to Equation (3.11), to get the following relation:

$$i \left( \frac{\partial^2 \phi}{\partial x \partial t} \bar{\phi} - \phi \frac{\partial^2 \bar{\phi}}{\partial x \partial t} \right) - \frac{\beta}{2} \left( \frac{\partial^3 \phi}{\partial x^3} \bar{\phi} + \phi \frac{\partial^3 \bar{\phi}}{\partial x^3} \right) + 3\gamma |\phi|^2 \frac{\partial}{\partial x} (|\phi|^2) = 0. \quad (3.12)$$

Subtracting Equation (3.9) from Equation (3.12) gives the following equation:

$$i \frac{\partial}{\partial t} \left( \frac{\partial \phi}{\partial x} \bar{\phi} - \phi \frac{\partial \bar{\phi}}{\partial x} \right) - \frac{\beta}{2} \frac{\partial}{\partial x} \left( \frac{\partial^2 \phi}{\partial x^2} \bar{\phi} + \phi \frac{\partial^2 \bar{\phi}}{\partial x^2} \right) + \beta \frac{\partial}{\partial x} \left( |\frac{\partial \phi}{\partial x}|^2 \right) + 2\gamma |\phi|^2 \frac{\partial}{\partial x} (|\phi|^2) = 0. \quad (3.13)$$

By integrating Equation (3.13) with respect to  $x$  and by using the boundary condition in Equation (3.3), the following relation is obtained:

$$\frac{\partial}{\partial t} \int_{-\infty}^{\infty} i \left( \frac{\partial \phi}{\partial x} \bar{\phi} - \phi \frac{\partial \bar{\phi}}{\partial x} \right) dx = 0,$$

which leads to the momentum conservation law

$$\int_{-\infty}^{\infty} i \left( \frac{\partial \phi}{\partial x} \bar{\phi} - \phi \frac{\partial \bar{\phi}}{\partial x} \right) dx = \text{constant}.$$

### 3.3 | Energy conservation law

$$\int_{-\infty}^{\infty} \left[ \frac{\beta}{2} \left| \frac{\partial \phi}{\partial x} \right|^2 + \frac{\gamma}{2} |\phi|^4 \right] dx = \text{constant}. \quad (3.14)$$

*Proof.* To prove Equation (3.14), multiply the NLSE (1.1) by  $\frac{\partial \bar{\phi}}{\partial t}$  and its complex conjugate by  $\frac{\partial \phi}{\partial t}$  as follows:

$$i \frac{\partial \phi}{\partial t} \frac{\partial \bar{\phi}}{\partial t} - \frac{\beta}{2} \frac{\partial^2 \phi}{\partial x^2} \frac{\partial \bar{\phi}}{\partial t} + \gamma \frac{\partial \bar{\phi}}{\partial t} \phi |\phi|^2 = 0, \quad (3.15)$$

$$-i \frac{\partial \phi}{\partial t} \frac{\partial \bar{\phi}}{\partial t} - \frac{\beta}{2} \frac{\partial \phi}{\partial t} \frac{\partial^2 \bar{\phi}}{\partial x^2} + \gamma \bar{\phi} \frac{\partial \phi}{\partial t} |\phi|^2 = 0. \quad (3.16)$$

Then add Equation (3.15) to Equation (3.16) to obtain the following equation:

$$-\frac{\beta}{2} \left[ \frac{\partial}{\partial x} \left( \frac{\partial \phi}{\partial x} \frac{\partial \bar{\phi}}{\partial t} + \frac{\partial \phi}{\partial t} \frac{\partial \bar{\phi}}{\partial x} \right) - \frac{\partial}{\partial t} \left( \left| \frac{\partial \phi}{\partial x} \right|^2 \right) \right] + \frac{\gamma}{2} \frac{\partial}{\partial t} (|\phi|^2 |\phi|^2) = 0. \quad (3.17)$$

Now, integrating Equation (3.17) with respect to  $x$  with the use of boundary condition in Equation (3.3) gives the following relation:

$$\frac{\partial}{\partial t} \left[ \frac{\beta}{2} \int_{-\infty}^{\infty} \left| \frac{\partial \phi}{\partial x} \right|^2 dx + \frac{\gamma}{2} \int_{-\infty}^{\infty} |\phi|^4 dx \right] = 0,$$

which implies that the following energy conservation law is satisfied:

$$\int_{-\infty}^{\infty} \left[ \frac{\beta}{2} \left| \frac{\partial \phi}{\partial x} \right|^2 + \frac{\gamma}{2} |\phi|^4 \right] dx = \text{constant}.$$

## 4 | NUMERICAL METHOD

In this section, the NLSE (1.1) in the presence of CD,  $\beta$ , and SPM,  $\gamma$ , that takes the following form

$$i \frac{\partial \phi}{\partial t} - \frac{\beta}{2} \frac{\partial^2 \phi}{\partial x^2} + \gamma |\phi|^2 \phi = 0, \quad x_L \leq x \leq x_R, \quad t \geq 0, \quad (4.1)$$

with the following initial condition

$$\phi(x, 0) = g(x), \quad (4.2)$$

and the boundary condition

$$\frac{\partial \phi}{\partial x}(x, t) = 0, \quad \text{at } x = x_L, x_R, \quad (4.3)$$

is solved numerically by using Crank–Nicolson method, where  $\phi(x, t)$  is the complex slowly varying pulse envelope,  $t$  represents the time variable,  $x$  denotes to position variable, and  $x_L$  and  $x_R$  are real numbers.

To implement the numerical method, impose that the complex function  $\phi(x, t)$  has the following form:

$$\phi(x, t) = v(x, t) + iw(x, t), \quad (4.4)$$

where  $v(x, t)$  and  $w(x, t)$  are real functions,<sup>27,32</sup> thus, the boundary condition (4.3) becomes on the following form:

$$\frac{\partial v}{\partial x}(x, t) = \frac{\partial w}{\partial x}(x, t) = 0, \quad \text{when } x = x_L, x_R. \quad (4.5)$$

Substitute Equation (4.4) into Equation (4.1) and separate the imaginary and real parts of the resulting equation respectively as follows:

$$\frac{\partial v}{\partial t} - \frac{\beta}{2} \frac{\partial^2 w}{\partial x^2} + \gamma(v^2 + w^2)w = 0, \quad (4.6)$$

$$\frac{\partial w}{\partial t} + \frac{\beta}{2} \frac{\partial^2 v}{\partial x^2} - \gamma(v^2 + w^2)v = 0. \quad (4.7)$$

Equations (4.6) and (4.7) can be written as follows:

$$\frac{\partial}{\partial t} \begin{bmatrix} v \\ w \end{bmatrix} - \frac{\beta}{2} \begin{pmatrix} 0 & 1 \\ -1 & 0 \end{pmatrix} \frac{\partial^2}{\partial x^2} \begin{bmatrix} v \\ w \end{bmatrix} + \gamma \begin{pmatrix} 0 & v^2 + w^2 \\ -(v^2 + w^2) & 0 \end{pmatrix} \begin{bmatrix} v \\ w \end{bmatrix} = \mathbf{0},$$

where  $\mathbf{0}$  is  $2 \times 1$  zero vector.

Let

$$\boldsymbol{\phi} = \begin{bmatrix} v \\ w \end{bmatrix}, A = \begin{pmatrix} 0 & 1 \\ -1 & 0 \end{pmatrix}, G(\boldsymbol{\phi}) = \begin{pmatrix} 0 & v^2 + w^2 \\ -(v^2 + w^2) & 0 \end{pmatrix},$$

and thus, Equations (4.6) and (4.7) take the following form:

$$\frac{\partial \boldsymbol{\phi}}{\partial t} - \frac{\beta}{2} A \frac{\partial^2 \boldsymbol{\phi}}{\partial x^2} + \gamma G(\boldsymbol{\phi}) \boldsymbol{\phi} = \mathbf{0}. \quad (4.8)$$

## 4.1 | Space discretization

In order to develop a numerical method for solving the system given in Equation (4.8), suppose that the region  $R = [x_L < x < x_R] \times [t > 0]$  with its boundary  $\partial R$  consisting of the ordinates  $x = x_L, x = x_R$ , and the axis  $t = 0$  is covered with a rectangular mesh of points with the following coordinates:

$$x = x_m = x_L + (m - 1)h,$$

$$h = \frac{x_R - x_L}{N - 1}, \quad m = 1, 2, \dots, N,$$

where  $N$  is the number of points in the grid and  $h$  is the distance between any two consecutive points.

Then approximate the exact solutions  $v(x_m, t) = v_m$  and  $w(x_m, t) = w_m$ , by the approximation solutions  $V(x_m, t) = V_m$  and  $W(x_m, t) = W_m$ , respectively. Also, approximate the second derivative in Equation (4.8) by the following central difference formula:

$$\left[ \frac{\partial^2 v(x, t)}{\partial x^2} \right]_{(x=x_m, t)} = \frac{1}{h^2} [\delta_x^2 v]_{(x=x_m, t)} + O(h^2),$$

where

$$[\delta_x^2 v]_{(x=x_m, t)} = v(x_m + h, t) - 2v(x_m, t) + v(x_m - h, t),$$

or briefly, it can be written as follows:

$$\frac{\partial^2 v_m}{\partial x^2} = \frac{1}{h^2} (v_{m+1} - 2v_m + v_{m-1}) + O(h^2). \quad (4.9)$$

Similarly, the central difference formula of  $w(x, t)$  takes the following form:

$$\frac{\partial^2 w_m}{\partial x^2} = \frac{1}{h^2} [\delta_x^2 w]_{(x=x_m, t)} + O(h^2) = \frac{1}{h^2} (w_{m+1} - 2w_m + w_{m-1}) + O(h^2). \quad (4.10)$$

Now, substitute Equations (4.9) and (4.10) into Equations (4.6) and (4.7) to get the following correlations:

$$\dot{V}_m - \frac{\beta}{2h^2} (W_{m+1} - 2W_m + W_{m-1}) + \gamma(V_m^2 + W_m^2)W_m = 0, \quad m = 1, 2, \dots, N, \quad (4.11)$$

$$\dot{W}_m + \frac{\beta}{2h^2} (V_{m+1} - 2V_m + V_{m-1}) - \gamma(V_m^2 + W_m^2)V_m = 0, \quad (4.12)$$

which can be written as follows:

$$\dot{\Phi}_m - \frac{\beta}{2h^2} A \delta_x^2 \Phi_m + \gamma G(\Phi_m) \Phi_m = \mathbf{0}, \quad (4.13)$$

where the error term is dropped after using the approximation solutions  $V$  and  $W$ ,  $\mathbf{0}$  is  $2N \times 1$  zero vector, and

$$\Phi = \begin{bmatrix} V \\ W \end{bmatrix}.$$

In addition, the boundary condition equation (4.3) is approximated by the central difference formula as follows:

$$\begin{aligned} \frac{\partial V_m}{\partial x} &= \frac{1}{2h} (V_{m+1} - V_{m-1}) = 0, \\ \frac{\partial W_m}{\partial x} &= \frac{1}{2h} (W_{m+1} - W_{m-1}) = 0, \text{ when } m = 1, N, \end{aligned} \quad (4.14)$$

where  $x_1 = x_L$  and  $x_N = x_R$  that imply the following relations:

$$V_0 = V_2, W_0 = W_2, V_{N+1} = V_{N-1}, W_{N+1} = W_{N-1}. \quad (4.15)$$

By using the boundary condition equation (4.15), Equations (4.11) and (4.12) which represent a system of  $2N$  equations can be written as follows:

$$\dot{\Phi} + [S + B(\Phi)]\Phi = \mathbf{0}, \quad (4.16)$$

where

$$\Phi = [\Phi_1^T, \Phi_2^T, \dots, \Phi_N^T]^T, \Phi_m = [V_m, W_m]^T, m = 1, 2, \dots, N.$$

$S$  and  $B(\Phi)$  are  $N \times N$  block tridiagonal matrices on the following form:

$$S = \frac{\beta}{2h^2} \begin{pmatrix} 2A & -2A & z & z & \cdots & z \\ -A & 2A & -A & z & \cdots & z \\ z & -A & \cdots & -A & \cdots & \vdots \\ \vdots & \cdots & \cdots & \cdots & \cdots & z \\ z & \cdots & z & -A & 2A & -A \\ z & z & \cdots & z & -2A & 2A \end{pmatrix}, B(\Phi) = \text{diag}[B_1(\Phi_1), B_2(\Phi_2), \dots, B_N(\Phi_N)],$$

$$B_m(\Phi_m) = \begin{pmatrix} 0 & \gamma(V_m^2 + W_m^2) \\ -\gamma(V_m^2 + W_m^2) & 0 \end{pmatrix}.$$

$z$  is  $2 \times 2$  zero matrix, and  $\mathbf{0}$  is  $2N \times 1$  zero vector.

## 4.2 | Time discretization

Assume that  $\Phi_m^n$  to be the fully discrete approximation to  $\Phi(x_m, t_n) = V(x_m, t_n) + iW(x_m, t_n)$ , where

$$t_n = nk, n = 0, 1, 2, \dots,$$

and  $k$  is the increment of time.

By using the following implicit point rule for the integration in time of the system in Equation (4.16),

$$\Phi_m^n = \frac{\Phi_m^{n+1} + \Phi_m^n}{2}, m = 1, 2, \dots, N, \quad (4.17)$$

and by using the following forward difference for the derivatives with respect to time,

$$(\dot{\Phi})_m^n = \frac{\Phi_m^{n+1} - \Phi_m^n}{k} \quad (4.18)$$

when ignoring the truncation error  $O(k)$ . Therefore, the system in Equation (4.16) becomes on the following form:

$$\Phi^{n+1} - \Phi^n + k \left[ S + B \left( \frac{\Phi^{n+1} + \Phi^n}{2} \right) \right] \left( \frac{\Phi^{n+1} + \Phi^n}{2} \right) = \mathbf{0}, \quad (4.19)$$

which represents a block nonlinear tridiagonal system of  $2N$  nonlinear algebraic equations that can be solved by using Newton's method.

## 4.3 | Newton's method

The nonlinear system (4.19) can be written as follows<sup>25</sup>:

$$\mathbf{F}(\Phi) = \mathbf{0},$$

where  $\mathbf{0}$  is  $2N \times 1$  zero vector and

$$\mathbf{F}(\Phi) = [\mathbf{f}_1^T, \mathbf{f}_2^T, \dots, \mathbf{f}_N^T]^T, \mathbf{f}_m = [(f1)_m, (f2)_m]^T, \Phi = [\Phi_1^T, \Phi_2^T, \dots, \Phi_N^T]^T, \Phi_m = [V_m, W_m]^T, m = 1, 2, \dots, N,$$

where  $(f1)_m$  and  $(f2)_m$  are the nonlinear functions.

Newton's method can be applied as follows:

$$\Phi^{(j+1)} = \Phi^{(j)} - J^{-1}(\Phi^{(j)}) \mathbf{F}(\Phi^{(j)}), j = 0, 1, 2, \dots, \quad (4.20)$$

where  $j$  is the number of iteration and  $J$  is the Jacobian  $N \times N$  block tridiagonal matrix on the form

$$J(\Phi) = \begin{pmatrix} A_1 & C_1 & z & \cdots & z \\ B_2 & A_2 & \ddots & \ddots & \vdots \\ z & \ddots & \ddots & \ddots & z \\ \vdots & \ddots & \ddots & \ddots & C_{N-1} \\ z & \cdots & z & B_N & A_N \end{pmatrix},$$

where  $A$ ,  $B$ , and  $C$  are  $2 \times 2$  matrices on the following form:

$$A_i = \begin{pmatrix} \frac{\partial(f1)_i}{\partial V_i} & \frac{\partial(f1)_i}{\partial W_i} \\ \frac{\partial(f2)_i}{\partial V_i} & \frac{\partial(f2)_i}{\partial W_i} \end{pmatrix}, i = 1, 2, \dots, N; B_i = \begin{pmatrix} \frac{\partial(f1)_i}{\partial V_{i-1}} & \frac{\partial(f1)_i}{\partial W_{i-1}} \\ \frac{\partial(f2)_i}{\partial V_{i-1}} & \frac{\partial(f2)_i}{\partial W_{i-1}} \end{pmatrix}, i = 2, 3, \dots, N; C_i = \begin{pmatrix} \frac{\partial(f1)_i}{\partial V_{i+1}} & \frac{\partial(f1)_i}{\partial W_{i+1}} \\ \frac{\partial(f2)_i}{\partial V_{i+1}} & \frac{\partial(f2)_i}{\partial W_{i+1}} \end{pmatrix}, i = 1, 2, \dots, N-1.$$

The system (4.20) can be calculated as follows: firstly, introduce the  $2N \times 1$  vector  $\mathbf{y}$  to satisfy the following relation:

$$J(\Phi^{(j)})\mathbf{y} = \mathbf{F}(\Phi^{(j)}), \quad j = 0, 1, \dots, \quad (4.21)$$

which can be obtained by using Gauss elimination to solve the block tridiagonal system in Equation (4.21). Secondly, substitute the vector  $\mathbf{y}$  in the following relation:

$$\Phi^{(j+1)} = \Phi^{(j)} - \mathbf{y} \quad (4.22)$$

to update the initial guess vector  $\Phi^{(j)}$ . Thus, Equations (4.21) and (4.22) are applied until the following relation is satisfied:

$$\|\Phi^{(j+1)} - \Phi^{(j)}\|_\infty < tol, \quad (4.23)$$

where  $tol$  is a small prescribed value to measure the errors.

The efficiency of the numerical method depends on its stability and accuracy which will be proven and discussed in the two following sections.

## 5 | THE ACCURACY OF THE SCHEME

The order of accuracy of a numerical method refers to how rapidly errors decrease in the limit as the step size tends to zero. To study the accuracy of the implicit finite difference method used in this study, substitute Equations (4.17) and (4.18) into the system (4.13) to get

$$\frac{\phi_m^{n+1} - \phi_m^n}{k} - \frac{\beta}{2h^2} A \delta_x^2 \left( \frac{\phi_m^{n+1} + \phi_m^n}{2} \right) + \gamma g \left( \frac{\phi_m^{n+1} + \phi_m^n}{2} \right) = \mathbf{0}, \quad (5.1)$$

where

$$G(\phi_m)\phi_m = g(\phi_m).$$

Use Taylor's series expansion of all terms in Equation (5.1) about  $\phi_m^n$  where it is the exact solution vector of the NLSE to obtain the following expansions:

$$\begin{aligned}\boldsymbol{\phi}_m^{n+1} &= \left[ \boldsymbol{\phi} + k \frac{\partial \boldsymbol{\phi}}{\partial t} + \frac{k^2}{2!} \frac{\partial^2 \boldsymbol{\phi}}{\partial t^2} + O(k^3) \right]_m^n, \\ \boldsymbol{\phi}_{m\pm 1}^n &= \left[ \boldsymbol{\phi} \pm h \frac{\partial \boldsymbol{\phi}}{\partial x} + \frac{h^2}{2!} \frac{\partial^2 \boldsymbol{\phi}}{\partial x^2} \pm \frac{h^3}{3!} \frac{\partial^3 \boldsymbol{\phi}}{\partial x^3} + \frac{h^4}{4!} \frac{\partial^4 \boldsymbol{\phi}}{\partial x^4} + O(h^5) \right]_m^n, \\ \boldsymbol{\phi}_{m+1}^{n+1} &= \sum_{p=0}^{\infty} \frac{1}{p!} \left[ h \frac{\partial}{\partial x} + k \frac{\partial}{\partial t} \right]^p \boldsymbol{\phi}_m^n, \\ \boldsymbol{\phi}_{m-1}^{n+1} &= \sum_{p=0}^{\infty} \frac{1}{p!} \left[ k \frac{\partial}{\partial t} - h \frac{\partial}{\partial x} \right]^p \boldsymbol{\phi}_m^n,\end{aligned}$$

where

$$\begin{aligned}\delta_x^2 \boldsymbol{\phi}_m^n &= \boldsymbol{\phi}_{m+1}^n - 2\boldsymbol{\phi}_m^n + \boldsymbol{\phi}_{m-1}^n, \\ \delta_x^2 \boldsymbol{\phi}_m^{n+1} &= \boldsymbol{\phi}_{m+1}^{n+1} - 2\boldsymbol{\phi}_m^{n+1} + \boldsymbol{\phi}_{m-1}^n,\end{aligned}$$

which gives

$$\begin{aligned}\delta_x^2 \boldsymbol{\phi}_m^n &= \left[ h^2 \frac{\partial^2 \boldsymbol{\phi}}{\partial x^2} + \frac{1}{12} h^4 \frac{\partial^4 \boldsymbol{\phi}}{\partial x^4} \right]_m^n + \dots, \\ \delta_x^2 \boldsymbol{\phi}_m^{n+1} &= \left[ h^2 \frac{\partial^2 \boldsymbol{\phi}}{\partial x^2} + kh^2 \frac{\partial^3 \boldsymbol{\phi}}{\partial x^2 \partial t} + \frac{k^2 h^2}{2} \frac{\partial^4 \boldsymbol{\phi}}{\partial x^2 \partial t^2} + \frac{k^4}{12} \frac{\partial^4 \boldsymbol{\phi}}{\partial t^4} + \frac{h^4}{12} \frac{\partial^4 \boldsymbol{\phi}}{\partial x^4} \right]_m^n + \dots,\end{aligned}$$

and thus, the following expansions are gotten:

$$\frac{\boldsymbol{\phi}_m^{n+1} - \boldsymbol{\phi}_m^n}{k} = \left[ \frac{\partial \boldsymbol{\phi}}{\partial t} + \frac{k}{2} \frac{\partial^2 \boldsymbol{\phi}}{\partial t^2} + \frac{k^2}{3!} \frac{\partial^3 \boldsymbol{\phi}}{\partial t^3} + O(k^3) \right]_m^n, \quad (5.2)$$

$$\frac{1}{4h^2} \delta_x^2 (\boldsymbol{\phi}_m^{n+1} + \boldsymbol{\phi}_m^n) = \left[ \frac{1}{2} \frac{\partial^2 \boldsymbol{\phi}}{\partial x^2} + \frac{k}{4} \frac{\partial^3 \boldsymbol{\phi}}{\partial x^2 \partial t} + \frac{h^2}{24} \frac{\partial^4 \boldsymbol{\phi}}{\partial x^4} + \frac{kh^2}{48} \frac{\partial^5 \boldsymbol{\phi}}{\partial x^4 \partial t} + \frac{k^2}{8} \frac{\partial^4 \boldsymbol{\phi}}{\partial x^2 \partial t^2} + O(k^2 h^2 + k^3) \right]_m^n, \quad (5.3)$$

$$\mathbf{g} \left( \frac{\boldsymbol{\phi}_m^{n+1} + \boldsymbol{\phi}_m^n}{2} \right) = \mathbf{g}(\boldsymbol{\phi}_m^n) + \frac{k}{2} \frac{\partial \mathbf{g}(\boldsymbol{\phi}_m^n)}{\partial t} + \frac{k^2}{4} \frac{\partial^2 \mathbf{g}(\boldsymbol{\phi}_m^n)}{\partial t^2} + O(k^3). \quad (5.4)$$

Then substituting Equations (5.2)–(5.4) into Equation (5.1) gives

$$\begin{aligned}T_m^n &= \left[ \frac{\partial \boldsymbol{\phi}}{\partial t} - \frac{\beta}{2} A \frac{\partial^2 \boldsymbol{\phi}}{\partial x^2} + \gamma \mathbf{g}(\boldsymbol{\phi}) \right]_m^n + \frac{k}{2} \frac{\partial}{\partial t} \left[ \frac{\partial \boldsymbol{\phi}}{\partial t} - \frac{\beta}{2} A \frac{\partial^2 \boldsymbol{\phi}}{\partial x^2} + \gamma \mathbf{g}(\boldsymbol{\phi}) \right]_m^n \\ &\quad + \left[ \frac{k^2}{3!} \frac{\partial^3 \boldsymbol{\phi}}{\partial t^3} - \beta A \left( \frac{h^2}{24} \frac{\partial^2 \boldsymbol{\phi}}{\partial x^4} + \frac{kh^2}{48} \frac{\partial^5 \boldsymbol{\phi}}{\partial t \partial x^4} + \frac{k^2}{8} \frac{\partial^4 \boldsymbol{\phi}}{\partial x^2 \partial t^2} \right) + \gamma \frac{\partial^2 \mathbf{g}(\boldsymbol{\phi})}{\partial t^2} \right]_m^n + O(K^2 h^2 + k^3 + h^4),\end{aligned}$$

where  $T_m^n$  is the truncation error.

Since that  $\boldsymbol{\phi}$  is the exact solution vector of Equation (1.1), then the first and second brackets are equal to zero, from Equation (4.8). Therefore, the truncation error becomes on the following form:

$$T_m^n = O(K^2 + kh^2 + h^2), \quad (5.5)$$

which proves that the numerical scheme used is second order in time and space.<sup>20,25</sup>

## 6 | THE STABILITY OF THE SCHEME

The stability analysis can be done to see for what values of approximation variables allow the errors in the solution to be bounded. A finite difference scheme is stable if the errors made at one time step of the calculation do not cause the errors to be magnified as the computations are continued. Von-Neuman stability analysis is used to prove the stability of our numerical scheme, given as follows:

Assume that

$$\Phi_m^n = H^n \mathbf{u} \exp \{i\mu m h\} \quad (6.1)$$

is the test function, where  $i = \sqrt{-1}$ ,  $\mu \in R$ ,  $\mathbf{u} \in R^2$ , and  $H \in R^{2 \times 2}$  is the amplification matrix.<sup>25</sup> The necessary condition for stability of the difference scheme is

$$\max_j |\lambda_j| \leq 1, j = 1, 2 \quad (6.2)$$

where  $\lambda_j$  are the eigenvalues of the amplification matrix  $H$ . In order to apply von-Neumann stability analysis, the differential equation (4.13) must be used in the following linearized form:

$$\frac{\partial \Phi}{\partial t} - \frac{\beta}{2} A \frac{\partial^2 \Phi}{\partial x^2} + \rho A \Phi = \mathbf{0}, \quad (6.3)$$

where

$$\rho = \max \{ \gamma(v^2 + w^2) \}.$$

The implicit scheme for Equation (6.3) can be written as

$$\Phi_m^{n+1} - \Phi_m^n + \frac{k}{2h^2} \left( \frac{-\beta}{2h^2} A \delta_x^2 + \rho A \right) (\Phi_m^{n+1} + \Phi_m^n) = \mathbf{0}, \quad (6.4)$$

and find the derivatives in this scheme to get the following relation:

$$\delta_x^2 \Phi_m^n = -4 \sin^2 \left( \frac{\mu h}{2} \right) H^n \mathbf{u} \exp \{ i\mu m h \}. \quad (6.5)$$

Then substituting Equations (6.1) and (6.5) into Equation (6.4) gives the following relation:

$$\begin{aligned} & H^{n+1} \mathbf{u} \exp \{ i\mu m h \} - H^n \mathbf{u} \exp \{ i\mu m h \} + \frac{k\beta}{h^2} A \sin^2 \left( \frac{\mu h}{2} \right) H^{n+1} \mathbf{u} \exp \{ i\mu m h \} \\ & + \frac{k\beta}{h^2} A \sin^2 \left( \frac{\mu h}{2} \right) H^n \mathbf{u} \exp \{ i\mu m h \} + \frac{k\rho A}{2} H^{n+1} \mathbf{u} \exp \{ i\mu m h \} + \frac{k\rho A}{2} H^n \mathbf{u} \exp \{ i\mu m h \} = \mathbf{0}. \end{aligned} \quad (6.6)$$

By influencing Equation (6.6) by  $\mathbf{u}^{-1}$  from the right-hand side and then multiplying by  $\exp \{ -i\mu m h \}$ , the following correlation is obtained:

$$H^{n+1} \mathbf{I}_1 - H^n \mathbf{I}_1 + \frac{k\beta}{h^2} \sin^2 \left( \frac{\mu h}{2} \right) A H^{n+1} \mathbf{I}_1 + \frac{k\beta}{h^2} \sin^2 \left( \frac{\mu h}{2} \right) A H^n \mathbf{I}_1 + \frac{k\rho}{2} A H^{n+1} \mathbf{I}_1 + \frac{k\rho}{2} A H^n \mathbf{I}_1 = \mathbf{0}, \quad (6.7)$$

$$\mathbf{I}_1 = \begin{bmatrix} 1 \\ 0 \end{bmatrix}.$$

Then multiply Equation (6.7) by the transpose vector  $\mathbf{I}_1^T = [1 \ 0]$  from the right-hand side to get the following relation:

$$H^{n+1} - H^n + \frac{k\beta}{h^2} \sin^2\left(\frac{\mu h}{2}\right) A H^{n+1} + \frac{k\beta}{h^2} \sin^2\left(\frac{\mu h}{2}\right) A H^n + \frac{k\rho}{2} A H^{n+1} + \frac{k\rho}{2} A H^n = 0. \quad (6.8)$$

After that, influence Equation (6.8) by  $(H^{n+1})^{-1}$  from the right-hand side to obtain the following equation:

$$(I + \theta A)H - (I - \theta A) = z, \quad (6.9)$$

where  $I$  is  $2 \times 2$  identity matrix,  $z$  is  $2 \times 2$  zero matrix, and

$$\frac{k}{2} \left[ \frac{2\beta}{h^2} \sin^2\left(\frac{\mu h}{2}\right) + \rho \right] = \theta.$$

Thus, the matrix  $H$  can be given explicitly as

$$H = (I + \theta A)^{-1}(I - \theta A),$$

so the eigenvalues of the matrix  $H$  are obtained by using Mathematica as follows:

$$\lambda_1 = \frac{1 - 2i\theta - \theta^2}{1 + \theta^2}, \quad \lambda_2 = \frac{1 + 2i\theta - \theta^2}{1 + \theta^2}.$$

Therefore,

$$|\lambda_1| = \frac{1 - 2i\theta - \theta^2}{1 + \theta^2} \cdot \frac{1 + 2i\theta - \theta^2}{1 + \theta^2} = 1.$$

Similarly, the modulus of the other eigenvalue  $|\lambda_2|$  is equal to one; that is,

$$|\lambda_j| = 1, j = 1, 2,$$

which concludes that the scheme is unconditionally stable on the time step size  $k$ , in the linear sense.<sup>28,29</sup>

## 7 | NUMERICAL RESULTS

This section displays various numerical results such as the conserved quantities, the maximum error  $L_\infty$ , and the summation of errors at each space step  $L_2$  in different cases.

### 7.1 | One soliton

In this case, the initial condition takes the following form<sup>9,34</sup>:

$$\phi(x) = \sqrt{\frac{2a}{\gamma}} \operatorname{sech}\left(\sqrt{\frac{-2a}{\beta}}x\right) \exp\left\{i\left(\frac{-c}{\beta}\right)x\right\}. \quad (7.1)$$

The conserved quantities are displayed in Table 1. The integrations in the conservation laws are calculated by using trapezoid rule as follows.

(i) Mass conservation law

$$\int_{x_L}^{x_R} |\phi|^2 dx \approx \frac{h}{2} \left[ v_1^2 + w_1^2 + 2 \sum_{i=2}^{N-1} (v_i^2 + w_i^2) + v_N^2 + w_N^2 \right]. \quad (7.2)$$

Since that mass is constant from Equations (3.1) and (7.2), mass conservation law becomes on the following form:

$$\frac{h}{2} \left[ v_1^2 + w_1^2 + 2 \sum_{i=2}^{N-1} (v_i^2 + w_i^2) + v_N^2 + w_N^2 \right] = \text{constant}. \quad (7.3)$$

(ii) Momentum conservation law

$$i \int_{x_L}^{x_R} \left( \bar{\phi} \frac{\partial \phi}{\partial x} - \frac{\partial \bar{\phi}}{\partial x} \phi \right) dx = 2 \int_{x_L}^{x_R} \left( w \frac{\partial v}{\partial x} - v \frac{\partial w}{\partial x} \right),$$

where  $\frac{\partial v}{\partial x}, \frac{\partial w}{\partial x}$  are approximated by using the relation in Equation (4.14). Then apply the trapezoid rule and the boundary condition in Equation (4.14) to calculate momentum from the following relation:

$$i \int_{x_L}^{x_R} \left( \bar{\phi} \frac{\partial \phi}{\partial x} - \frac{\partial \bar{\phi}}{\partial x} \phi \right) dx \approx \sum_{i=2}^{N-1} \{ w_i(v_{i+1} - v_{i-1}) - v_i(w_{i+1} - w_{i-1}) \}. \quad (7.4)$$

Since that momentum is conserved from Equations (3.6) and (7.4), this equation becomes on the following form:

$$\sum_{i=2}^{N-1} \{ w_i(v_{i+1} - v_{i-1}) - v_i(w_{i+1} - w_{i-1}) \} = \text{constant}. \quad (7.5)$$

(iii) Energy conservation law

$$\int_{x_L}^{x_R} \left[ \frac{\beta}{2} \left| \frac{\partial \phi}{\partial x} \right|^2 + \frac{\gamma}{2} |\phi|^4 \right] dx = \int_{x_L}^{x_R} \left[ \frac{\beta}{2} \left( \left( \frac{\partial v}{\partial x} \right)^2 + \left( \frac{\partial w}{\partial x} \right)^2 \right) + \frac{\gamma}{2} (v^2 + w^2)^2 \right] dx.$$

Then by using the boundary condition in Equation (4.14) and trapezoid rule, energy can be obtained from the following relation:

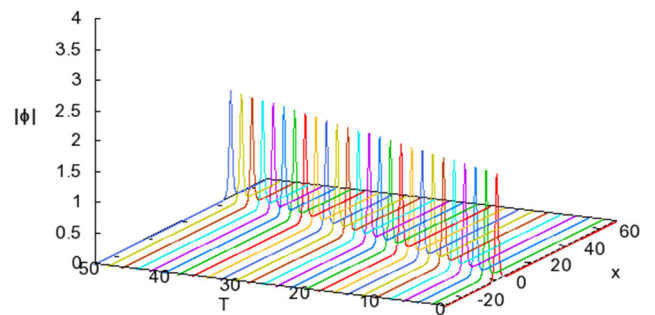


**FIGURE 1** One soliton with the parameters  $h = 0.05$ ,  $k = 0.01$ ,  $\gamma = 2/3$ ,  $\beta = -1.0$ ,  $c = 1$ ,  $a = 1$ ,  $\text{tol} = 10^{-6}$ ,  $x_L = -30$ ,  $x_R = 70$  [Colour figure can be viewed at [wileyonlinelibrary.com](http://wileyonlinelibrary.com)]

$$\int_{x_L}^{x_R} \left[ \frac{\beta}{2} \left| \frac{\partial \phi}{\partial x} \right|^2 + \frac{\gamma}{2} |\phi|^4 \right] dx \approx \frac{\beta}{8h} \sum_{i=2}^{N-1} [(v_{i+1} - v_{i-1})^2 + (w_{i+1} - w_{i-1})^2] + \frac{\gamma h}{4} \left\{ (v_1^2 + w_1^2)^2 + 2 \sum_{i=2}^{N-1} (v_i^2 + w_i^2)^2 + (v_N^2 + w_N^2)^2 \right\}. \quad (7.6)$$

Since that energy is constant from Equations (3.14) and (7.6), this equation becomes on the following form:

$$\frac{\beta}{8h} \sum_{i=2}^{N-1} [(v_{i+1} - v_{i-1})^2 + (w_{i+1} - w_{i-1})^2] + \frac{\gamma h}{4} \left\{ (v_1^2 + w_1^2)^2 + 2 \sum_{i=2}^{N-1} (v_i^2 + w_i^2)^2 + (v_N^2 + w_N^2)^2 \right\} = \text{constant}. \quad (7.7)$$

Likewise, the accuracy of the scheme at some parameters is displayed in Table 1 by calculating the maximum error  $L_\infty$  and the total of errors  $L_2$  at different values of the time step  $k$  by using the following relations:

$$L_\infty = \|ER\|_\infty = \max_{1 < m < N} \{ |\|\phi(x_m, t_n)\| - \|V_m^n + iW_m^n\|| \},$$

$$L_2 = \|ER\|_2 = \left\{ \sum_{m=1}^N [|\|\phi(x_m, t_n)\| - \|V_m^n + iW_m^n\||^2] \right\}^{\frac{1}{2}}.$$

## 7.2 | Soliton like periodic and dissipative wave

This wave takes the following form:

$$\phi(x, t) = \frac{\sqrt{s} \exp \{-ist\}}{\sqrt{4s-\gamma} + \sqrt{s} \cosh \left( 2x \sqrt{\frac{s}{-\beta}} \right)}, \quad (7.8)$$

from which the initial condition is given by the following relation:

$$\phi(x, t) = \frac{\sqrt{s}}{\sqrt{4s-\gamma} + \sqrt{s} \cosh \left( 2x \sqrt{\frac{s}{-\beta}} \right)}, \quad (7.9)$$

where the angular velocity  $s$  has the following form:

$$s = -a - \frac{c^2}{2\beta}.$$

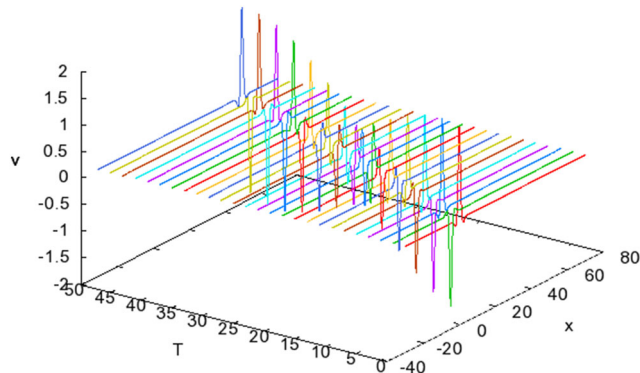
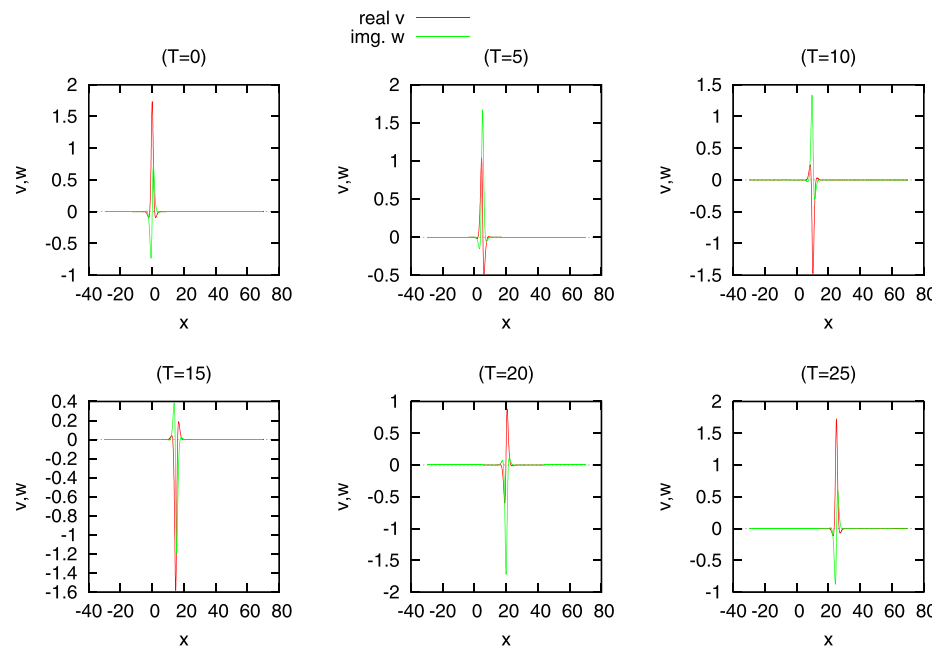
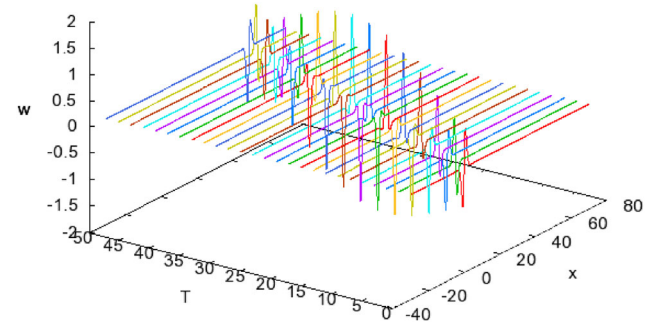


FIGURE 2 The real part  $V$  in one soliton with the parameters  $h = 0.05$ ,  $k = 0.01$ ,  $\gamma = 2/3$ ,  $\beta = -1.0$ ,  $c = 1$ ,  $a = 1$ ,  $tol = 10^{-6}$ ,  $x_L = -30$ ,  $x_R = 70$  [Colour figure can be viewed at [wileyonlinelibrary.com](http://wileyonlinelibrary.com)]

## 8 | DISCUSSION

Equation (1) is solved numerically by using the implicit Crank–Nicolson scheme which is a second-order accuracy in space and time and unconditionally stable. For one soliton solution in Equation (7.1), the behavior of the soliton and its real and imaginary parts are shown in Figures 1–4. It was noted that it represents a localized soliton moves without any changes in its shape and direction. Also, mass, momentum, and energy are conservative as in Table 1. Since Equation (1.1) state characterized the nonlinearity and dispersion contributions in the fiber mode, the values of  $\beta$  and  $\gamma$  controlled the stability state in this mode. For ( $\beta \gamma < 0$ ), Equation (1.1) behaves as a stable modulation

**FIGURE 3** The imaginary part  $W$  in one soliton with the parameters  $h = 0.05$ ,  $k = 0.01$ ,  $\gamma = 2/3$ ,  $\beta = -1.0$ ,  $c = 1$ ,  $a = 1$ ,  $tol = 10^{-6}$ ,  $x_L = -30$ ,  $x_R = 70$  [Colour figure can be viewed at [wileyonlinelibrary.com](http://wileyonlinelibrary.com)]



**FIGURE 4** The real and imaginary parts  $V$ ,  $W$  in one soliton with the parameters  $h = 0.05$ ,  $k = 0.01$ ,  $\gamma = 2/3$ ,  $\beta = -1.0$ ,  $c = 1$ ,  $a = 1$ ,  $tol = 10^{-6}$ ,  $x_L = -30$ ,  $x_R = 70$  [Colour figure can be viewed at [wileyonlinelibrary.com](http://wileyonlinelibrary.com)]

**TABLE 1** One soliton with the parameters  $h = 0.05$ ,  $k = 0.01$ ,  $\gamma = 2/3$ ,  $\beta = -1.0$ ,  $c = 1$ ,  $a = 1$ ,  $tol = 10^{-6}$ ,  $x_L = -30$ ,  $x_R = 70$

Time	Mass	Momentum	Energy	$L_2$	$L_\infty$
10	4.242638664	-8.474637187	0.6949355552	0.09631796673	0.01618961974
20	4.242638664	-8.474633626	0.6949350961	0.1906182830	0.03158822098
30	4.242638664	-8.474630290	0.6949439394	0.2851346062	0.04689921796
40	4.242638664	-8.474612276	0.6949304997	0.3800942897	0.06254107432
50	4.242638664	-8.474616966	0.6949405563	0.4748621177	0.07813227748

mode while for  $(0 < \beta \gamma)$ , an unstable wave can be propagated in this medium. To examine the effects of  $\beta$  and  $\gamma$  on the wave properties, we choose another initial solution in Equation (7.9) which gives different behaviors according to  $\beta$  and  $\gamma$  values. For example, the soliton variations with space and time in the stable regime are plotted in Figures 5 and 6. It was reported that by increasing time, the soliton amplitude decreases and soliton width

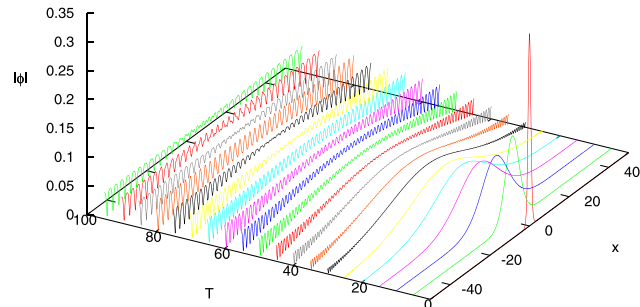


**FIGURE 5** Modulus of the wave with the parameters  $h = 0.05$ ,  $k = 0.01$ ,  $\gamma = 2/3$ ,  $\beta = -0.5$ ,  $c = 1.0$ ,  $a = 0.2$ ,  $tol = 10^{-6}$ ,  $x_L = -50$ ,  $x_R = 50$  [Colour figure can be viewed at [wileyonlinelibrary.com](http://wileyonlinelibrary.com)]

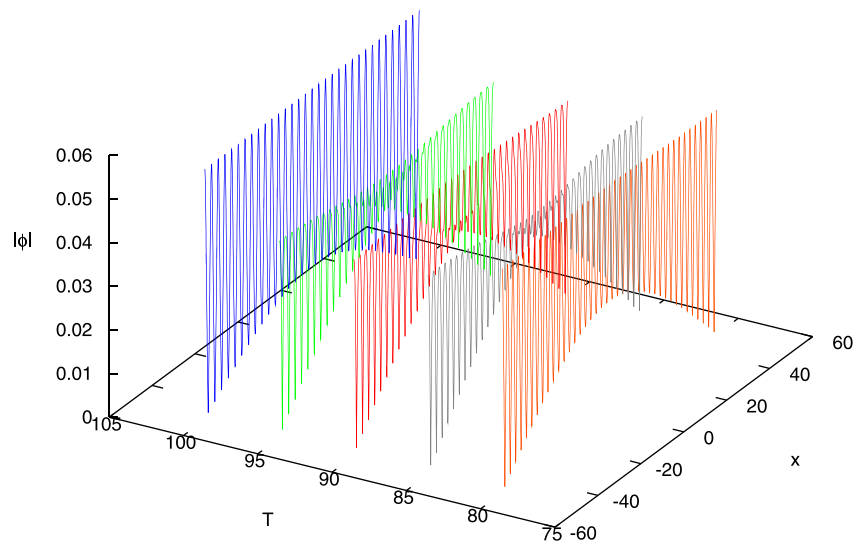


**FIGURE 6** Modulus of the wave with the parameters  $h = 0.05$ ,  $k = 0.01$ ,  $\gamma = 2/3$ ,  $\beta = -0.5$ ,  $c = 1.0$ ,  $a = 0.2$ ,  $tol = 10^{-6}$ ,  $x_L = -50$ ,  $x_R = 50$  [Colour figure can be viewed at [wileyonlinelibrary.com](http://wileyonlinelibrary.com)]

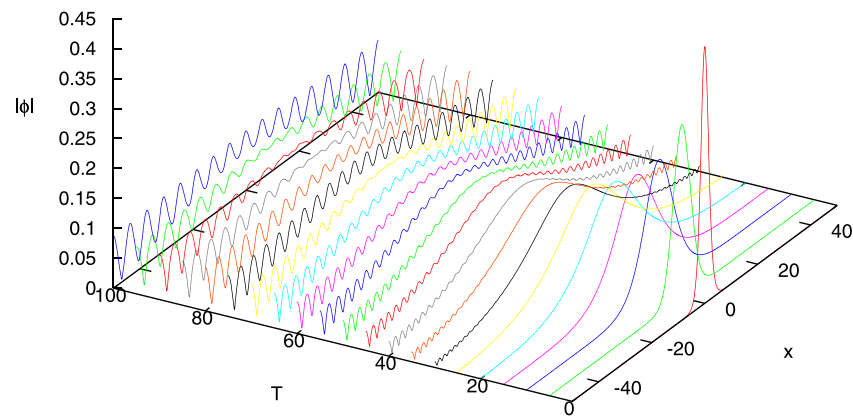


**FIGURE 7** Modulus of the wave with the parameters  $h = 0.05$ ,  $k = 0.01$ ,  $\gamma = 2/3$ ,  $\beta = -1.0$ ,  $c = 1.0$ ,  $a = 0.2$ ,  $tol = 10^{-6}$ ,  $x_L = -50$ ,  $x_R = 50$  [Colour figure can be viewed at [wileyonlinelibrary.com](http://wileyonlinelibrary.com)]

**FIGURE 8** Modulus of the wave with the parameters  $h = 0.05$ ,  $k = 0.01$ ,  $\gamma = 2/3$ ,  $\beta = -1.0$ ,  $c = 1.0$ ,  $a = 0.2$ ,  $tol = 10^{-6}$ ,  $x_L = -50$ ,  $x_R = 50$  [Colour figure can be viewed at [wileyonlinelibrary.com](http://wileyonlinelibrary.com)]

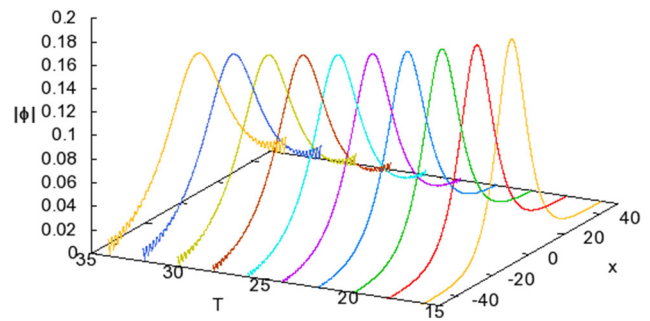


**FIGURE 9** Modulus of the wave with the parameters  $h = 0.05$ ,  $k = 0.01$ ,  $\gamma = 2/3$ ,  $\beta = -1.0$ ,  $c = 1.0$ ,  $a = 0.2$ ,  $tol = 10^{-6}$ ,  $x_L = -50$ ,  $x_R = 50$  [Colour figure can be viewed at [wileyonlinelibrary.com](http://wileyonlinelibrary.com)]

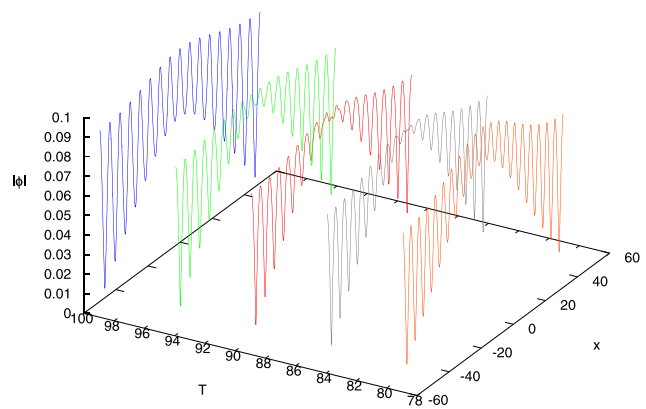


**FIGURE 10** Modulus of the wave with the parameters  $h = 0.05$ ,  $k = 0.01$ ,  $\gamma = 2/3$ ,  $\beta = 0.5$ ,  $c = 1.0$ ,  $a = 0.2$ ,  $tol = 10^{-6}$ ,  $x_L = -50$ ,  $x_R = 50$  [Colour figure can be viewed at [wileyonlinelibrary.com](http://wileyonlinelibrary.com)]

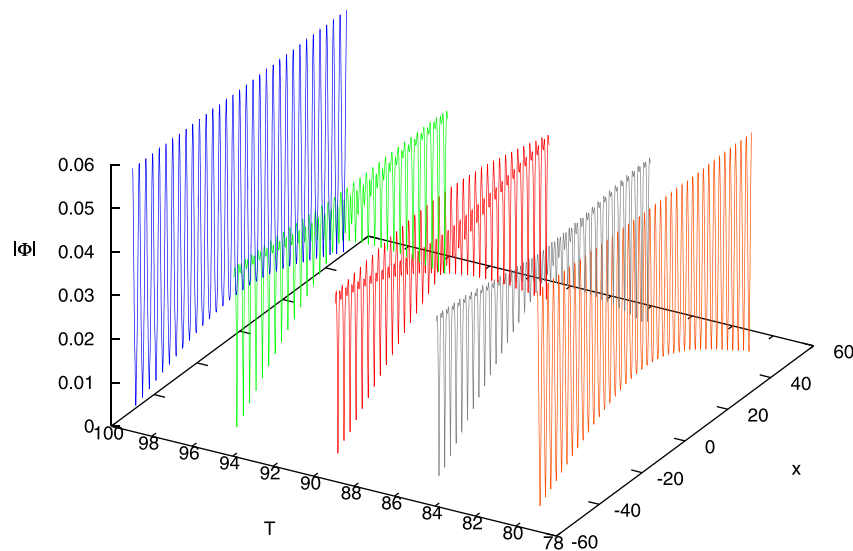
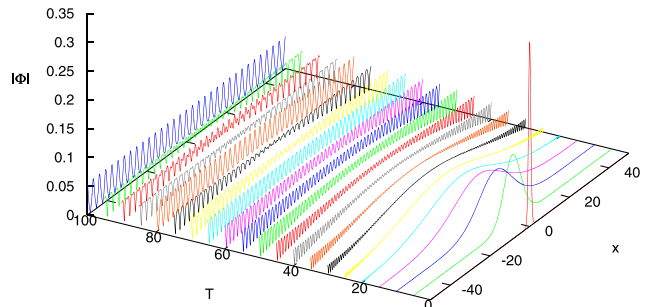


**FIGURE 11** Modulus of the wave with the parameters  $h = 0.05$ ,  $k = 0.01$ ,  $\gamma = 2/3$ ,  $\beta = 0.5$ ,  $c = 1.0$ ,  $a = 0.2$ ,  $tol = 10^{-6}$ ,  $x_L = -50$ ,  $x_R = 50$  [Colour figure can be viewed at [wileyonlinelibrary.com](http://wileyonlinelibrary.com)]

increases. After time 20, the soliton inverted partially to a periodic behavior, with large values of time the wave behavior becomes as an envelope soliton view; see Figure 6. Furthermore, the increase of negative values of  $\beta$  increases the soliton amplitude and decreases its width as shown in Figures 7–9. Also, the periodic wave amplitude

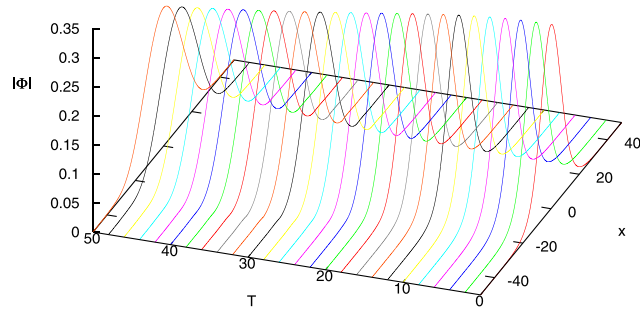


**FIGURE 12** Modulus of the wave with the parameters  $h = 0.05$ ,  $k = 0.01$ ,  $\gamma = 0.0151745$ ,  $\beta = 1.42349$ ,  $c = 1.0$ ,  $a = -0.3289575$ ,  $tol = 10^{-6}$ ,  $x_L = -50$ ,  $x_R = 50$  [Colour figure can be viewed at [wileyonlinelibrary.com](http://wileyonlinelibrary.com)]

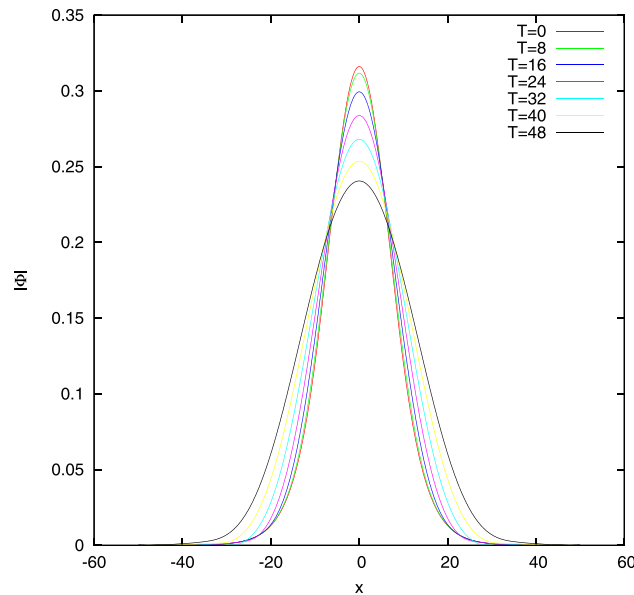


**FIGURE 13** Modulus of the wave with the parameters  $h = 0.05$ ,  $k = 0.01$ ,  $\gamma = 0.0151745$ ,  $\beta = 1.42349$ ,  $c = 1.0$ ,  $a = -0.3289575$ ,  $tol = 10^{-6}$ ,  $x_L = -50$ ,  $x_R = 50$  [Colour figure can be viewed at [wileyonlinelibrary.com](http://wileyonlinelibrary.com)]

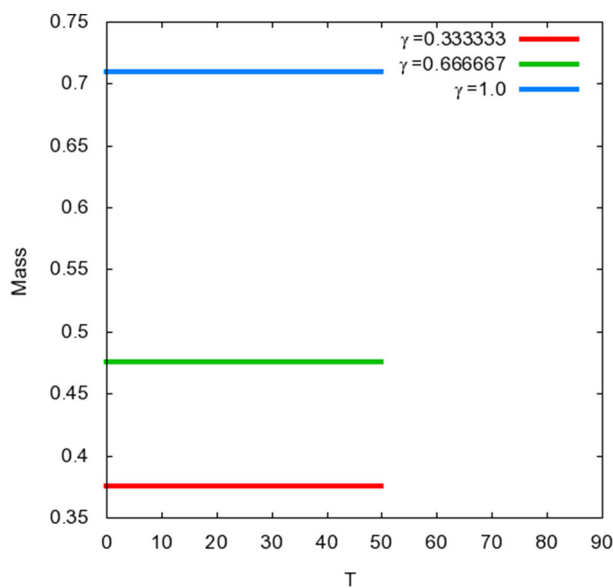


**FIGURE 14** Mass versus  $\gamma$  in the wave when  $h = 0.05$ ,  $k = 0.01$ ,  $\beta = -1.0$ ,  $c = 1.0$ ,  $a = 0.2$ ,  $tol = 10^{-6}$ ,  $x_L = -50$ ,  $x_R = 50$  [Colour figure can be viewed at [wileyonlinelibrary.com](http://wileyonlinelibrary.com)]

increases. The positive value of  $\beta$  remains the periodic waves stable and behaves as conidial waves as shown in Figures 10 and 11. Moreover, the reduction in the parameter  $\gamma$  and increase of the positive parameter  $\beta$  tend to remain the localized soliton shape with the increase of time. The only change is reduction of localized soliton amplitude and the raise of its width without any periodic formation as shown in Figures 12 and 13. On the other hand, for the initial solution in Equation (7.9), the effects of  $\beta$  and  $\gamma$  parameters on mass and energy are depicted on Figures 14–17. It was introduced that the mass and energy are conservative. The mass and energy values depend on the wave type generated for given values. Finally, the length of soliton like periodic and dissipative wave variations with  $\beta$  and  $\gamma$  values is shown in Figures 18 and 19. In summary, the optical physical parameters  $\beta$  and  $\gamma$  are very effective on the type production and generations of solitary and envelope optical waves.

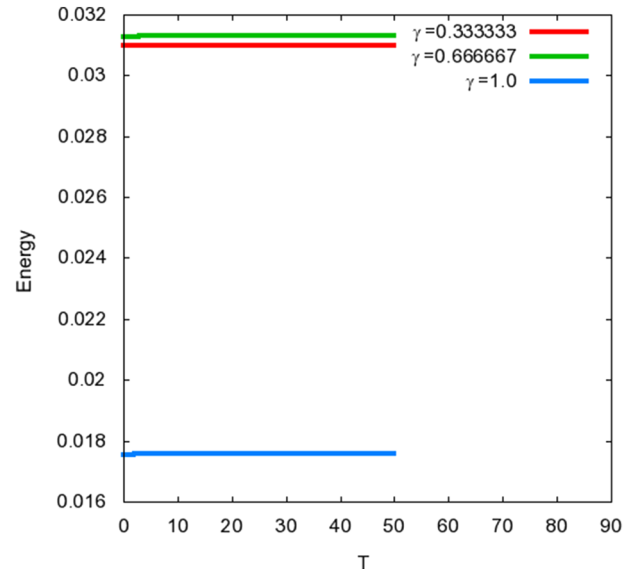


**FIGURE 15** Energy versus  $\gamma$  in the wave when  $h = 0.05$ ,  $k = 0.01$ ,  $\beta = -1.0$ ,  $c = 1.0$ ,  $a = 0.2$ ,  $tol = 10^{-6}$ ,  $x_L = -50$ ,  $x_R = 50$  [Colour figure can be viewed at [wileyonlinelibrary.com](http://wileyonlinelibrary.com)]

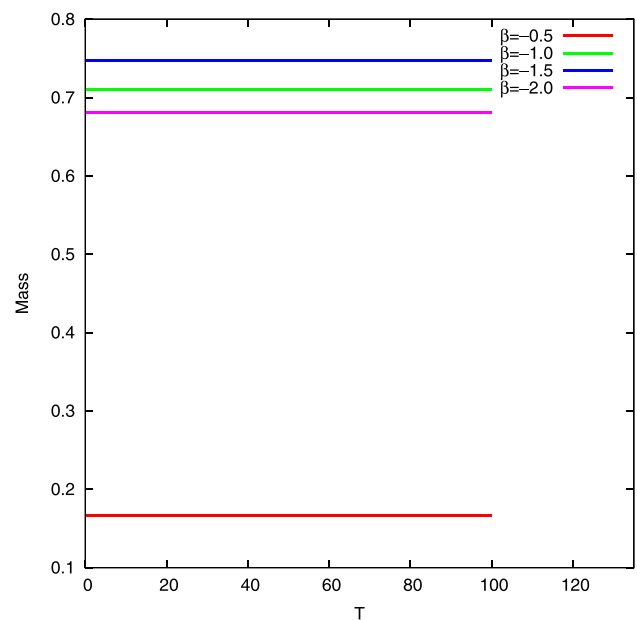


**FIGURE 16** Mass versus  $\beta$  in the wave when  $h = 0.05$ ,  $k = 0.01$ ,  $\gamma = 1.0$ ,  $c = 1.0$ ,  $a = 0.2$ ,  $tol = 10^{-6}$ ,  $x_L = -50$ ,  $x_R = 50$  [Colour figure can be viewed at [wileyonlinelibrary.com](http://wileyonlinelibrary.com)]

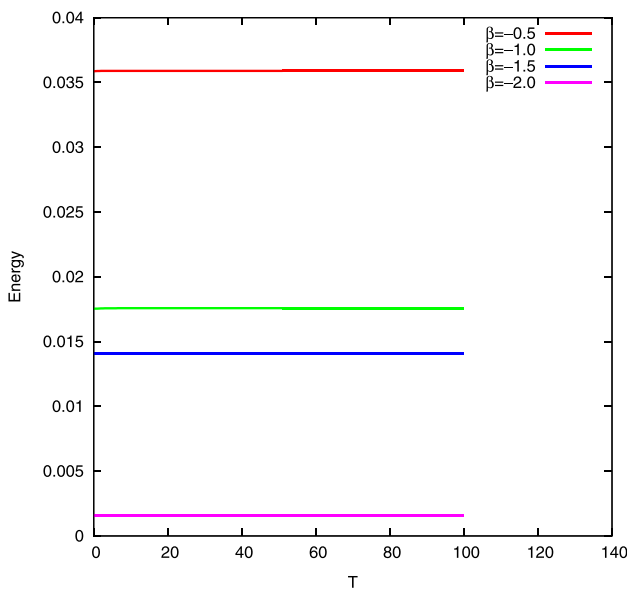


**FIGURE 17** Energy versus  $\beta$  in the wave when  $h = 0.05$ ,  $k = 0.01$ ,  $\gamma = 1.0$ ,  $c = 1.0$ ,  $a = 0.2$ ,  $tol = 10^{-6}$ ,  $x_L = -50$ ,  $x_R = 50$  [Colour figure can be viewed at [wileyonlinelibrary.com](http://wileyonlinelibrary.com)]

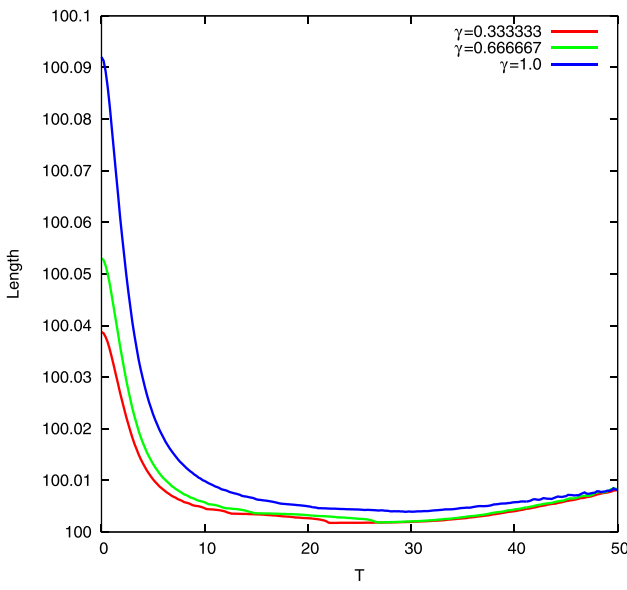


**FIGURE 18** Length versus  $\gamma$  in the wave when  $h = 0.05$ ,  $k = 0.01$ ,  $\beta = -1.0$ ,  $c = 1.0$ ,  $a = 0.2$ ,  $tol = 10^{-6}$ ,  $x_L = -50$ ,  $x_R = 50$  [Colour figure can be viewed at [wileyonlinelibrary.com](http://wileyonlinelibrary.com)]

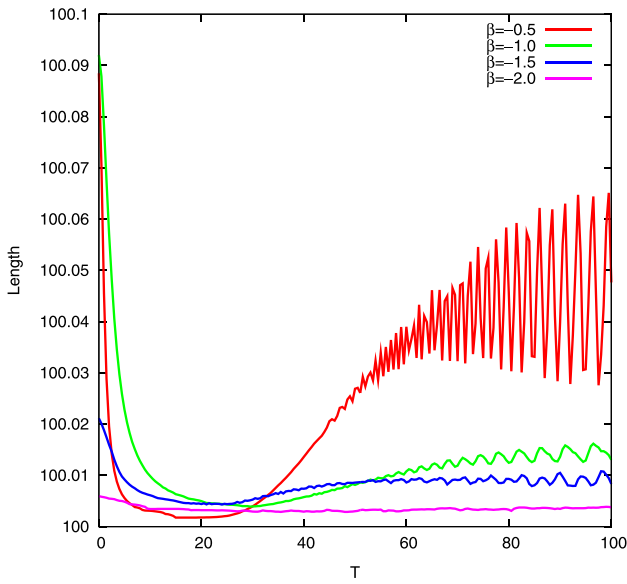


**FIGURE 19** Length versus  $\beta$  in the wave when  $h = 0.05$ ,  $k = 0.01$ ,  $\gamma = 1.0$ ,  $c = 1.0$ ,  $a = 0.2$ ,  $tol = 10^{-6}$ ,  $x_L = -50$ ,  $x_R = 50$  [Colour figure can be viewed at [wileyonlinelibrary.com](http://wileyonlinelibrary.com)]

## 9 | CONCLUSION

We have derived a computer code for the resulting implicit scheme of solving the NLSE by using Crank–Nicolson method, which is second order in space and time and unconditionally stable. The constancy of the quantities mass, momentum, and energy with time has proved the strength of the simulation. We have found that the CD and SPM factors influence on the conserved quantities and these effects lower depending on the increase or decrease in the factors' values in the case of one soliton. Moreover, the soliton moves smoothly without any distortion in its configuration. On the other hand, for the example of soliton like periodic and dissipative wave, the CD and SPM factors are operative on controlling the solitary type existence optical modes.

## CONFLICT OF INTEREST

This work does not have any conflict of interest.

## ORCID

Sultan Z. Alamri  <https://orcid.org/0000-0003-4621-9158>

## REFERENCES

1. Felice D. A study of a nonlinear Schrödinger equation for optical fibers. *Ph.D. Thesis*: University Of Florence, Italia; 2016.
2. Mitschke F, Mahrke C, Hause A. Soliton content of fiber-optic light pulses. *Appl Sci*. 2017;7(6):635.
3. Triki H, Bensalem C, Biswas A, et al. Self-similar optical solitons with continuous-wave background in a quadratic–cubic non-centrosymmetric waveguide. *Optics Commun*. 2019;437:392–398.
4. Nakkeeran K. Bright and dark optical solitons in fiber media with higher-order effects. *Chaos Solitons Fractals*. 2002;13(4):673–679.
5. Serkin VN, Hasegawa A. Novel soliton solutions of the nonlinear Schrödinger equation model. *Phys Rev Lett*. 2000;85(21):4502.
6. McDonald GD, Kuhn CarlosCN, Hardman KS, et al. Bright solitonic matter-wave interferometer. *Phys Rev Lett*. 2014;113(1):13002.
7. Dai C-Q, Wang X-G, Zhou G-Q, et al. Stable light-bullet solutions in the harmonic and parity-time-symmetric potentials. *Phys Rev A*. 2014;89(1):13834.
8. Triki H, Wazwaz A-M. Soliton solutions of the cubic-quintic nonlinear Schrödinger equation with variable coefficients. *Rom J Phys*. 2016;61(3-4):360.
9. Wazwaz A-M. Bright and dark optical solitons for (2+1)-dimensional Schrödinger (NLS) equations in the anomalous dispersion regimes and the normal dispersive regimes. *Optik*. 2019;192:162948.
10. Wazwaz A-M, Kaur L. Optical solitons for nonlinear Schrödinger (NLS) equation in normal dispersive regimes. *Optik*. 2019;184:428–435.
11. Wazwaz A-M, Xu G-Q. Bright, dark and Gaussons optical solutions for fourth-order Schrödinger equations with cubic–quintic and logarithmic nonlinearities. *Optik*. 2020;202:163564.
12. Abdelrahman MAE, Sohaly MA. Solitary waves for the nonlinear Schrödinger problem with the probability distribution function in the stochastic input case. *Eur Phys J Plus*. 2017;132(8):339.
13. Abdelrahman MAE, Abdo NF. On the nonlinear new wave solutions in unstable dispersive environments. *Physica Scripta*. 2020;95(4):45220.
14. Inc M, Aliyu AI, Yusuf A, Baleanu D. Optical and singular solitary waves to the PNLSE with third order dispersion in Kerr media via two integration approaches. *Optik*. 2018;163:142–151.
15. Agrawal GP. *Nonlinear Fiber Optics*. 4th ed. New York: Academic Press; 2007.
16. İnç M, Aliyu AI, Yusuf A, Baleanu D. Optical solitons and modulation instability analysis of an integrable model of (2+1)-dimensional Heisenberg ferromagnetic spin chain equation. *Superlattices Microstructures*. 2017;112:628–638.
17. Ghanbari B. A new generalized exponential rational function method to find exact special solutions for the resonance nonlinear Schrödinger equation. *Eur Phys J Plus*. 2018;133(4):142.
18. Inc M, Aliyu AI, Yusuf A, Baleanu D. Gray optical soliton, linear stability analysis and conservation laws via multipliers to the cubic nonlinear Schrödinger equation. *Optik*. 2018;164:472–478.
19. Houwe A, Inc M, Doka SY, Akinlar MA, Baleanu D. Chirped solitons in negative index materials generated by Kerr nonlinearity. *Results in Physics*. 2020;17:103097.
20. Wu H, Wang J, Liu X, Colmenares E, Yan G. The time accuracy analysis of Crank–Nicolson predictor-corrector numerical scheme for diffusion equations. *Numer Anal Methods Eng*. 2013;1:123.
21. İnç M, Aliyu AI, Yusuf A, Baleanu D. Novel optical solitary waves and modulation instability analysis for the coupled nonlinear Schrödinger equation in monomode step-index optical fibers. *Superlattices Microstruct*. 2018;113:745–753.
22. İnç M, Aliyu AI, Yusuf A, Baleanu D. Optical solitons, conservation laws and modulation instability analysis for the modified nonlinear Schrödinger's equation for Davydov solitons. *J Electromagnet Waves Appl*. 2018;32(7):858–873.
23. Baleanu D, Inc M, Yusuf A, Aliyu AI. Lie symmetry analysis, exact solutions and conservation laws for the time fractional Caudrey–Dodd–Gibbon–Sawada–Kotera equation. *Commun Nonlin Sci Numer Simul*. 2018;59:222–234.

24. Inc M, Yusuf A, Aliyu AI, Baleanu D. Lie symmetry analysis, explicit solutions and conservation laws for the space-time fractional nonlinear evolution equations. *Phys A: Stat Mech Appl.* 2018;496:371-383.
25. Alamri SZ. A numerical study of coupled nonlinear Schrodinger equation. *Master's Thesis:* King Abdulaziz University, Saudi Arabia; 2003.
26. Eskar R, Huang P, Feng X. A new high-order compact ADI finite difference scheme for solving 3D nonlinear Schrödinger equation. *Adv Differ Equa.* 2018;2018(1):1-15.
27. Ismail MS, Alamri SZ. Highly accurate finite difference method for coupled nonlinear Schrödinger equation. *Int J Comput Math.* 2004; 81(3):333-351.
28. Choy YY, Tan WN, Tay KG, Ong CT. Crank–Nicolson implicit method for the nonlinear Schrodinger equation with variable coefficient. *AIP Conf Proc.* 2014;1605:76-82.
29. Shojaei I, Rahami H. A closed-form solution for two-dimensional diffusion equation using Crank-Nicolson finite difference method. *J Algorit Comput.* 2019;51(1):71-77.
30. Bakodah HO, Al-Mazmumy M, Almuhalbedi SO. Solving system of integro differential equations using discrete adomian decomposition method. *J Taibah Univ Sci.* 2019;13(1):805-812.
31. Griffiths DF, Mitchell AR, Morris JL. A numerical study of the nonlinear Schrödinger equation. *Comput Methods Appl Mech Eng.* 1984; 45:177-215.
32. Taha TR, Ablowitz MI. Analytical and numerical aspects of certain nonlinear evolution equations. II. Numerical, nonlinear Schrödinger equation. *J Comput Phys.* 1984;55(2):203-230.
33. Fadul Albar R. Numerical treatment of the nonlinear schrodinger equation. *Master's Thesis:* King Abdulaziz University, Saudi Arabia; 1996.
34. Debnath L. *Nonlinear Partial Differential Equations for Scientists and Engineers*. Berlin/Heidelberg, Germany: Springer Science & Business Media; 2010.

**How to cite this article:** Alanazi AA, Alamri SZ, Shafie S, Binti Mohd Puzi S. Solving nonlinear Schrodinger equation using stable implicit finite difference method in single-mode optical fibers. *Math Meth Appl Sci.* 2021; 1–26. <https://doi.org/10.1002/mma.7553>